

# GeoHCC: Local Geometry-Aware Hierarchical Context Compression for 3D Gaussian Splatting

Xuan Deng  
Harbin Institute of  
Technology, Peng Cheng  
Laboratory  
Shenzhen, China  
dengxuan168168@gmail.com

Xiandong Meng  
Peng Cheng Laboratory  
Shenzhen, China  
mengxd@pcl.ac.cn

Hengyu Man  
Harbin Institute of  
Technology  
Harbin, China  
manhengyu@hotmail.com

Qiang Zhu  
Peng Cheng Laboratory,  
Shenzhen, China  
zhuqiang@std.uestc.edu.cn

Tiange Zhang  
Peng Cheng Laboratory,  
Shenzhen, China  
zhangtg@pcl.ac.cn

Debin Zhao  
Harbin Institute of  
Technology  
Harbin, China  
dbzhao@hit.edu.cn

Xiaopeng Fan  
Harbin Institute of  
Technology, Peng Cheng  
Laboratory, Harbin  
Institute of Technology  
Suzhou Research Institute  
Harbin, China  
fxp@hit.edu.cn

## Abstract

Although 3D Gaussian Splatting (3DGS) enables high-fidelity real-time rendering, its prohibitive storage overhead severely hinders practical deployment. Recent anchor-based 3DGS compression schemes reduce redundancy through context modeling, yet overlook explicit geometric dependencies, leading to structural degradation and suboptimal rate-distortion performance. In this paper, we propose GeoHCC, a geometry-aware 3DGS compression framework that incorporates inter-anchor geometric correlations into anchor pruning and entropy coding for compact representation. We first introduce Neighborhood-Aware Anchor Pruning (NAAP), which evaluates anchor importance via weighted neighborhood feature aggregation and merges redundant anchors into salient neighbors, yielding a compact yet geometry-consistent anchor set. Building upon this optimized structure, we further develop a hierarchical entropy coding scheme, in which coarse-to-fine priors are exploited through a lightweight Geometry-Guided Convolution (GG-Conv) operator to enable spatially adaptive context modeling and rate-distortion optimization. Extensive experiments demonstrate that GeoHCC effectively resolves the structure preservation bottleneck, maintaining superior geometric integrity and rendering fidelity over state-of-the-art anchor-based approaches.

## CCS Concepts

• Computer vision; • Theory of computation; • Data compression.

## ACM Reference Format:

Xuan Deng, Xiandong Meng, Hengyu Man, Qiang Zhu, Tiange Zhang, Debin Zhao, and Xiaopeng Fan. 2018. GeoHCC: Local Geometry-Aware Hierarchical Context Compression for 3D Gaussian Splatting. In *Proceedings of Make sure to enter the correct conference title from your rights confirmation email (Conference acronym 'XX)*. ACM, New York, NY, USA, 10 pages. <https://doi.org/XXXXXXX.XXXXXXX>

2026-03-31 02:07. Page 1 of 1–10.

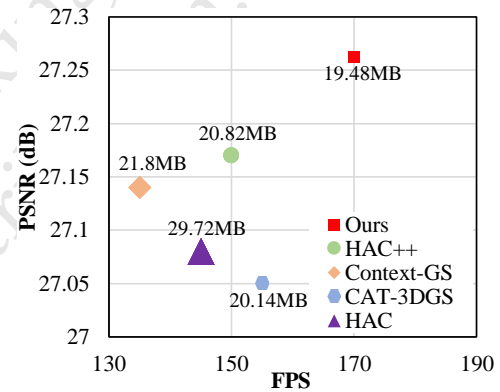


Figure 1: Trade-off between rendering FPS and PSNR for different methods. Marker size denotes storage cost, where smaller markers correspond to lower storage.

## 1 Introduction

3D Gaussian Splatting (3DGS) [18] has emerged as a powerful explicit 3D representation that models scenes with a set of anisotropic Gaussians with learnable attributes, including position, covariance, opacity, and spherical harmonics, enabling efficient optimization and high-quality novel-view synthesis. Its optimized rasterization supports fast convergence and real-time rendering, offering a strong alternative to implicit neural representations. However, high-quality reconstruction typically requires millions of primitives, leading to considerable storage and memory overhead. This redundancy hinders practical deployment, especially on resource-constrained platforms, and has motivated extensive research on compact 3DGS representations and compression.

Early 3DGS compression methods [10, 11, 13, 19, 21, 30, 38, 58] mainly reduce storage through primitive pruning or vector quantization. While effective, they focus on compressing attribute value of each individual gaussian and largely ignore the inherent geometric

correlation among Gaussians. Although such dependencies have been widely exploited in image and video compression [7, 15, 17, 22–24, 31–33, 44, 50], modeling them within 3DGS remains non-trivial due to the irregularly distribution of Gaussian primitives in 3D space. Locality-aware-GS [45] attempts to incorporate local geometric relations directly over massive unstructured Gaussian primitives, but the cost of neighborhood correlation search becomes prohibitive at large scale. Conversely, Anchor-based representations, e.g., Scaffold-GS [29], alleviate this issue by hierarchically clustering primitives around anchors and thus provide a more compact and structured representation. Nevertheless, Scaffold-GS treats anchors as isolated entities, leaving the local geometric correlations among neighboring anchors underexplored.

To further alleviate spatial redundancy, recent advances have incorporated more structured priors into anchor-based compression framework. Inspired by NeRF feature grids [14, 34, 36], HAC [4] and HAC++ [5] leverage hash grids for context modeling. Context-GS [47] takes a different approach by organizing anchors hierarchically to capture dependencies across representation levels, thus improving entropy modeling. Despite these advances, a fundamental limitation persists: current methods largely overlook the intrinsic geometric structures among anchors. Grid-based context models (e.g. HAC) rely on coarse extrinsic discretization and often fail to capture fine-grained geometric relationships in irregular anchor clouds. Hierarchical methods such as Context-GS [47], despite their stronger representational capacity, typically construct multi-level context structures on top of heuristic pruning strategies, such as opacity-based anchor removal. By directly discarding low-importance anchors, these methods may disrupt local geometric continuity and weaken the structural foundation required for reliable coarse-to-fine context prediction. Since finer levels can no longer inherit sufficiently stable geometric priors from the base layers, ultimately leading to suboptimal structure preservation and entropy estimation.

In this work, we argue that geometry-aware context modeling is crucial to unlocking the full compression potential of 3DGS. Rather than serving merely as attribute carriers, anchors are treated as nodes in a geometric graph where local neighborhoods exhibit strong geometric correlations. Based on this insight, we propose GeoHCC, a geometry-aware 3DGS compression framework that incorporates inter-anchor geometric correlations into anchor pruning and entropy coding for compact representation. We first introduce Neighborhood-Aware Anchor Pruning (NAAP), which evaluates anchor importance via graph aggregation and merges redundant anchors into salient neighbors. Building on the preserved local structure, we further design a hierarchical entropy coding scheme with geometry-guided indexed context. To implement this efficiently, we design a lightweight Geometry-Guided Convolution (GG-Conv) operator that aggregates contextual information from local geometric features, enabling the entropy model to learn spatially adaptive and geometry-consistent priors for more efficient compression. As shown in Figure 1, experiments on BungeeNerf [52] show that GeoHCC achieves a favorable FPS–PSNR trade-off than existing methods while requiring lower storage cost. Our main contributions are summarized as follows:

- We propose GeoHCC, a local geometry-aware hierarchical context compression framework for 3D Gaussian Splatting that reformulates anchor compression via geometry-induced graphs for consistent pruning and efficient hierarchical entropy modeling.
- To preserve the local geometric perception capability of anchors, we propose Neighborhood-Aware Anchor Pruning (NAAP), a graph-based adaptive sparsification strategy. By evaluating geometric importance and merging redundant anchors into their salient neighbors, NAAP preserves the inherent geometric correlation among anchors, producing a compact yet geometry-consistent representation with minimal fidelity loss.
- To exploit local geometric correlation in sparsified Gaussians, we propose hierarchical geometry-guided context modeling via a lightweight GG-Conv. By capturing spatially adaptive priors over irregular neighborhoods, our method achieves accurate probability estimation and state-of-the-art compression with high rendering quality.

## 2 Related Work

### 2.1 Graph-based 3D data modeling

Graph Signal Processing (GSP) [39, 53] provides a framework for analyzing signals on irregular domains by modeling data as nodes in a graph. In 3D vision, it has been widely applied to point cloud analysis (e.g., DGCNN [48] and PointNet++ [41, 42]), where local graphs encode geometric relations for feature aggregation. Similar principles have also been applied to point cloud compression, where exploiting inter-point correlations improves coding efficiency [8, 9, 12]. In this paper, we propose GeoHCC, which reformulates anchor-based 3DGS as an irregular geometric graph to jointly optimize anchor pruning and entropy coding via local geometry guidance, achieving significant bitrate reduction while preserving high-fidelity structural details.

### 2.2 Compact 3DGS Representation

3D Gaussian Splatting (3DGS) [18] achieves high-fidelity and efficient radiance field rendering, yet its explicit and unstructured Gaussian representation is less regular than the grid-based representations of NeRFs [2, 34, 51], leading to prohibitive storage overhead that necessitates advanced compression techniques.

Existing methods primarily tackle the storage challenge of 3D Gaussian Splatting by either reducing the number of primitives or learning compact attribute representations, without explicit rate-distortion optimization. Pruning-based approaches [1, 6, 10, 21, 27, 37, 40, 43] eliminate less contributive Gaussians using heuristic criteria, such as learnable masks, gradient magnitudes, or view-dependent significance. Complementary attribute compression techniques include spherical harmonics coefficient pruning [35] and vector quantization [13, 21, 46]. In addition to these primitive-level techniques, a representative anchor-based approach is Scaffold-GS [29], which uses anchor points to hierarchically distribute local 3D Gaussians and predicts their attributes on-the-fly conditioned on viewing direction and distance within the view frustum. Inspired by the anchor-based representation of Scaffold-GS [29], a series of recent works has focused on rate-distortion (RD) optimized

compression by improving entropy modeling through the exploitation of spatial or structural priors. These anchor-based methods have achieved impressive storage reduction while maintaining high rendering quality. For instance, HAC [4] and HAC++ [5] employ hash-grid-based spatial organization to derive compact context representations. Context-GS [47] and CompGS [28] further exploit hierarchical structure and anchor-primitive dependencies to improve entropy coding. Meanwhile, CAT-3DGS [54] adopts channel-wise autoregressive models to capture intra-attribute correlations, and Liu *et al.* [26] enhance density estimation through a Mixture-of-Priors formulation.

While these methods achieve impressive rate-distortion performance in 3D Gaussian Splatting compression, we argue that the core of effective compression lies in the entropy model. A well-designed entropy model can leverage local geometric correlations among anchors, enabling efficient coding and reducing storage requirements. However, current anchor-based 3DGS compression methods still have room for improvement in entropy model design, particularly in exploiting local geometric priors. Drawing inspiration from geometry-aware modeling in point cloud compression and graph neural networks, we propose a local geometry-aware entropy model. This model represents the unstructured anchor cloud as an irregular geometric graph and uses a lightweight Geometry-Guided Convolution (GG-Conv) to adaptively aggregate geometry-aware contextual priors from neighboring anchors.

## 3 Methodology

### 3.1 Preliminaries

**3D Gaussian Splatting (3DGS).** 3DGS [18] utilizes a collection of anisotropic 3D neural Gaussians to depict the scene so that the scene can be efficiently rendered using a tile-based rasterization technique. Beginning from a set of Structure-from-Motion (SfM) points, each Gaussian point is represented as follows:

$$G(\mathbf{p}) = \exp\left(-\frac{1}{2}(\mathbf{p} - \boldsymbol{\mu})^\top \boldsymbol{\Sigma}^{-1}(\mathbf{p} - \boldsymbol{\mu})\right), \quad (1)$$

where  $\mathbf{p}$  denotes the coordinates in the 3D scene, and  $\boldsymbol{\mu}$  and  $\boldsymbol{\Sigma}$  represent the mean position and covariance matrix of the Gaussian point, respectively. To ensure the positive semi-definiteness of  $\boldsymbol{\Sigma}$ , it is parameterized as  $\boldsymbol{\Sigma} = \mathbf{R}\mathbf{S}\mathbf{S}^\top\mathbf{R}^\top$ , where  $\mathbf{R}$  and  $\mathbf{S}$  denote the rotation and scaling matrices, respectively. Furthermore, each neural Gaussian possesses an opacity attribute  $\alpha \in \mathbb{R}^1$  and view-dependent color  $\mathbf{c} \in \mathbb{R}^3$ , modeled via spherical harmonics [56]. All attributes of the neural Gaussians, i.e.,  $\{\boldsymbol{\mu}, \mathbf{R}, \mathbf{S}, \alpha, \mathbf{c}\}$ , are learnable and optimized by minimizing the reconstruction loss of images rendered through tile-based rasterization.

### 3.2 Overview

Building upon the compact anchor-based representation of Scaffold-GS [29], we propose GeoHCC, a local geometry-aware hierarchical context compression framework for 3DGS, as illustrated in Figure 2. We define each anchor as a tuple  $\mathbf{a} = \{\mathbf{p}, \mathbf{f}, \mathbf{s}, \mathbf{o}\}$ , comprising position  $\mathbf{p} \in \mathbb{R}^3$ , feature  $\mathbf{f} \in \mathbb{R}^C$ , scaling factor  $\mathbf{s} \in \mathbb{R}^3$ , and offsets  $\mathbf{o} \in \mathbb{R}^{K \times 3}$ . The pipeline begins with anchor densification inherited from Scaffold-GS, which spawns additional anchors based on

view-space gradients to capture fine-grained scene details. To mitigate anchor redundancy and enhance the compression efficiency of 3DGS, we introduce the Neighborhood-Aware Anchor Pruning (NAAP) module (Sec. 3.3). Instead of relying on simple heuristic thresholding (e.g., fixed opacity values), NAAP constructs a local geometric graph to evaluate the importance of anchors in a neighborhood-aware manner and adaptively merges the attributes of redundant anchors into their salient neighbors, producing a compact yet locally geometry-consistent representation. Based on the pruned anchor set, we further organize the anchors into a multi-level hierarchy for efficient entropy coding. Specifically, we develop a hierarchical entropy coding scheme with geometry-guided context (Sec. 3.4). To enhance context modeling capability, we employ a lightweight Geometry-Guided Convolution (GG-Conv) that aggregates local geometric priors from the irregular neighborhood graph as coarse-grained information to guide finer-level entropy estimation. Finally, the decoded anchors generate 3D Gaussians via learnable offsets, achieving high-fidelity rasterization with extremely low storage overhead.

### 3.3 Neighborhood-Aware Anchor Pruning

Conventional 3DGS pruning strategies typically rely on point-wise attribute thresholds (e.g., opacity) to remove less important Gaussian anchors. However, such independent evaluation ignores local geometric distributions, may inadvertently eliminate structurally essential anchors, especially in low-density regions. To address this limitation, we propose Neighborhood-Aware Anchor Pruning (NAAP), which evaluates anchor importance within a local geometric neighborhood context and preserves structural continuity through adaptively merges redundant information. As illustrated in Figure 3, NAAP consists of four steps:

#### Step 1 & 2: Graph Construction and Importance Evaluation.

We initially construct a local geometric graph  $\mathcal{G} = (\mathcal{A}, \mathcal{E})$  to capture the local geometric correlations among anchors, where  $\mathcal{A} = \{\mathbf{a}_1, \dots, \mathbf{a}_N\}$  represents the set of anchors and  $\mathcal{E}$  denotes the edges connecting neighboring anchors, each anchor  $\mathbf{a}_i$  possesses a position  $\mathbf{p}_i$  and an accumulated average opacity  $\bar{\alpha}_i$ , which is derived by accumulating the opacity values of its associated neural Gaussians over  $N$  training iterations. We connect each anchor to its  $K$ -nearest neighbors within a radius  $r$ , forming the local neighborhood  $\mathcal{N}(i)$ , which provides a lightweight representation of local geometric structure for importance estimation.

To distinguish structurally essential anchors from noise or redundant anchors, we define a neighborhood-weighted importance score. Specifically, for each anchor (taking  $\mathbf{a}_i$  as an example), we first compute a distance-based weight  $w_{ij} = (\|\mathbf{p}_i - \mathbf{p}_j\|_2 + \epsilon)^{-1}$  between itself and its neighbor  $\mathbf{a}_j \in \mathcal{N}(i)$ , which assigns larger weights to closer neighbors. Then a smoothed neighborhood opacity  $\Phi_i$  is calculated to aggregate local context:

$$\Phi_i = \frac{\bar{\alpha}_i + \sum_{j \in \mathcal{N}(i)} w_{ij} \bar{\alpha}_j}{1 + \sum_{j \in \mathcal{N}(i)} w_{ij}}. \quad (2)$$

The final importance score  $\xi_i$  is formulated as a linear interpolation between the anchor-specific opacity and its neighborhood-aware observation:

$$\xi_i = (1 - \lambda)\bar{\alpha}_i + \lambda\Phi_i. \quad (3)$$

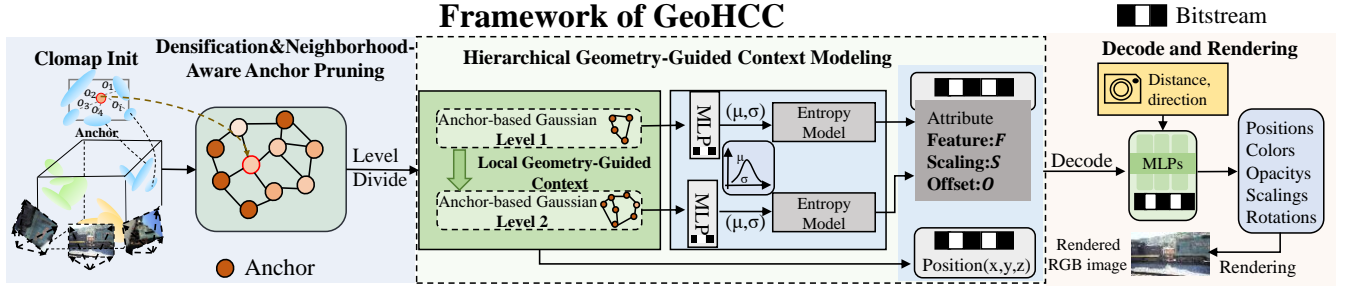


Figure 2: Overview of the proposed 3DGS compression framework. Starting with Colmap initialization, anchors first undergo densification to capture fine-grained scene details. To optimize the resulting structure, we introduce Neighborhood-Aware Anchor Pruning (NAAP), which constructs a local graph to evaluate geometric importance. Unlike simple removal, NAAP adaptively merges the attributes of redundant anchors into their salient neighbors, producing a compact yet locally geometry-consistent representation. Subsequently, the preserved anchors are organized into Hierarchical Geometry-Guided Context Modeling module, where we employ a Local Geometry-Guided Context to guide entropy coding. Finally, the decoded attributes (e.g., colors, opacities, scalings, rotations) generate 3D Gaussians via learnable offsets for high-fidelity rasterization.

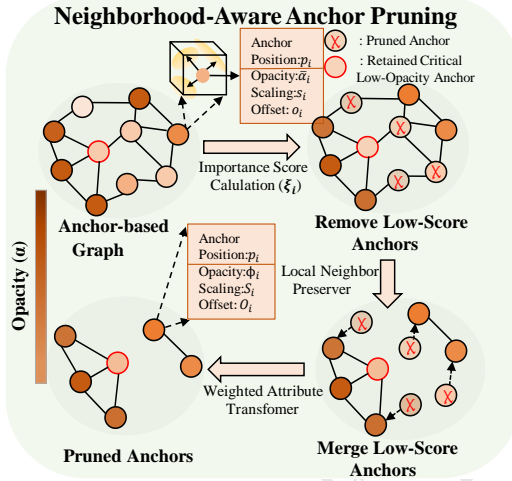


Figure 3: Neighborhood-Aware Anchor Pruning (NAAP) pipeline starts by constructing an anchor-based geometric graph, with nodes colored by average opacity (darker = higher). Importance scores ( $\xi_i$ ) are computed via neighborhood aggregation. Low-score anchors are identified as redundant and associated with their nearest salient neighbor (Local Neighbor Preserver). Instead of direct removal, a Weighted Attribute Transformer merges attributes from pruned anchors (opacity  $\bar{\alpha}_i$ , scaling  $s_i$ , offset  $o_i$ ) into the nearest retained anchor, yielding fused attributes ( $\phi_i, O_i, S_i$ , etc.) to preserve geometric and appearance information in a compact structure.

where  $\lambda \in [0, 1]$  is a balancing factor. Given a threshold  $\tau$ , we identify redundant anchors using the pruning mask:

$$\mathcal{M}_{prune} = \{\mathbf{a}_i \mid \xi_i < \tau\}. \quad (4)$$

This design enables anchors residing in structurally significant clusters to be preserved even if their individual opacity is relatively low.

**Step 3 & 4: Neighbor Association and Attribute Merging.** Unlike previous pruning strategies that directly discard anchors in  $\mathcal{M}_{prune}$ , we instead consolidate their information into the surviving geometry via a dedicated **Weighted Attribute Transformer**. For each redundant anchor  $\mathbf{a}_r \in \mathcal{M}_{prune}$ , we identify its nearest *salient neighbor*  $\mathbf{a}_k \in \mathcal{A} \setminus \mathcal{M}_{prune}$  as the target for information transfer. Let lowercase  $\theta \in \{\mathbf{o}, \mathbf{s}, \alpha\}$  and uppercase  $\Theta \in \{\mathbf{O}, \mathbf{S}, \phi\}$  denote the raw and fused attributes (offsets, scaling, and opacity), respectively. The transformation is governed by:

$$\Theta_k = (1 - \gamma)\theta_k + \gamma\theta_r, \quad (5)$$

where  $\gamma$  controls the contribution of the pruned anchor. This integration effectively condenses the geometric and appearance attributes of removed regions into their nearest neighbors ( $\theta \rightarrow \Theta$ ), ensuring that comprehensive scene information is preserved rather than lost. Finally, eliminating the anchors in  $\mathcal{M}_{prune}$  yields a compact, locally geometry-consistent representation.

As shown in Fig. 3, conventional threshold-based pruning would discard low-opacity anchors (highlighted by the red circle) induced by optimization noise. In contrast, NAAP can identify non-salient nodes within high-density clusters, which often play a crucial role in modeling key scene details during rendering.

### 3.4 Hierarchical Geometry-Guided Context Modeling

While hierarchical context models [25, 28, 47] have shown promising performance for anchor-based 3DGS compression, they often suffer from structural inefficiencies. Specifically, existing approaches typically rely on heuristic neighbor pooling or rigid spatial partitioning, which may fail to preserve precise geometric correspondence across hierarchy levels. As a result, the retrieved context is not always well-aligned with the query anchors, leading to sub-optimal entropy estimation. To overcome these limitations, we

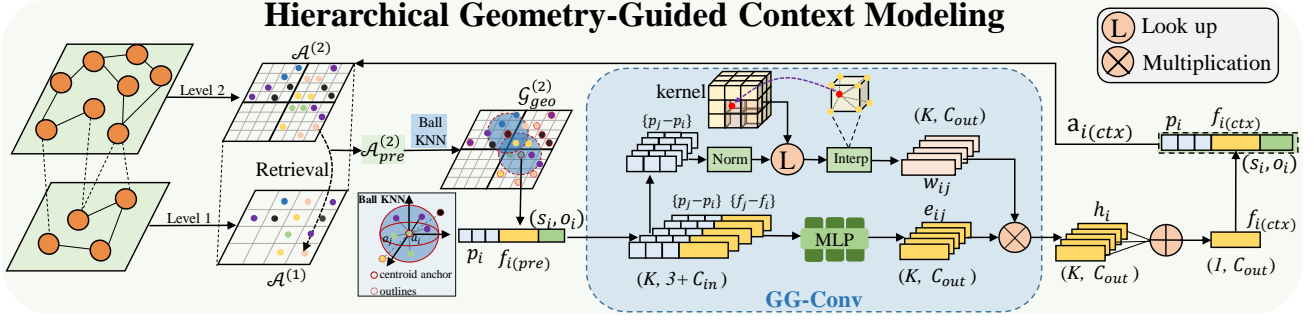


**Figure 4:** This module exploits cross-level correlations by mapping Level 1 attributes to Level 2 query anchors via a deterministic mapping  $\mathcal{M}$  to obtain the preliminary attributes  $\mathcal{A}_{pre}^{(2)}$ . Then, a  $k$ -NN graph is constructed over  $\mathcal{A}_{pre}^{(2)}$  to form the graph-based geometric prior  $\mathcal{G}_{geo}^{(2)}$ . Within the GG-Conv (dashed box): (1) **Geometry Branch:** Relative spatial offsets  $\Delta p_{ij}$  between the query anchor and its neighbors are used to query a learnable 3D kernel (Weight Look-up Table) via trilinear interpolation, generating dynamic geometric weights  $w_{ij}$  that explicitly encode the local spatial layout. (2) **Feature Branch:** This branch extracts semantic-geometric embeddings  $e_{ij}$  by transforming the concatenated residual features  $\Delta f_{ij}^{(1)}$  and relative offsets  $\Delta p_{ij}$  through an MLP  $\phi$ . Finally, the dynamic weights modulate these embeddings to produce the refined geometry-aware feature  $h_i$ , which provides a structured foundation for deriving the final local geometry-guided context  $a_{i(ctx)}$  for Level 2 attribute entropy coding.

propose a streamlined two-level autoregressive model that explicitly enforces geometric alignment between coarse and fine anchors. As shown in Figure 4, by strictly aligning the coarse geometry (Level 1) with fine attributes (Level 2), our method achieves precise context retrieval and refinement via a three-step process:

**1) Hierarchical Partitioning.** To leverage multi-scale spatial correlations, we organize the anchor set  $\mathcal{V}$  into a two-level hierarchy ( $\mathcal{L} = 2$ ) following Context-GS [47]. We first derive a coarse representation  $\mathcal{A}^{(1)}$  by quantizing anchor positions with a scaled voxel size  $\epsilon_1 = s \cdot \epsilon_0$ :

$$\mathcal{A}^{(1)} = \{a_j \in \mathcal{V} \mid j = \min\{i : \lfloor p_i / \epsilon_1 \rfloor\}\}, \quad (6)$$

where  $\epsilon_0$  is the initial fine-grained voxel size and  $\epsilon_1$  represents the coarse-grained resolution controlled by the scaling factor  $s$ . The fine level is then defined as  $\mathcal{A}^{(2)} = \mathcal{V} \setminus \mathcal{A}^{(1)}$  to ensure a disjoint structure. This hierarchy allows  $\mathcal{A}^{(1)}$  to serve as a coarse spatial prior for the entropy coding of  $\mathcal{A}^{(2)}$ .

**2) Inter-Level Context Retrieval.** To fully exploit the information provided by the coarse representation, we propose an inter-level retrieval strategy that transfers coarse-level attributes (e.g., feature  $f$ , scaling  $s$ , and offsets  $o$ ) to the fine-level query anchors, establishing a preliminary feature representation for subsequent geometric context refinement. This strategy utilizes the voxel grid as a spatial bridge to align attributes across levels. Specifically, based on the voxel partitioning rules in Eq. 6, we establish a deterministic mapping  $\mathcal{M}$  that associates each fine-level query anchor  $a_j^{(2)} \in \mathcal{A}^{(2)}$  with its corresponding coarse-level parent  $a_i^{(1)}$  within the same voxel, yielding a preliminary context set  $\mathcal{A}_{pre}^{(2)}$ :

$$\mathcal{A}_{pre}^{(2)} = \{(p_j^{(2)}, f_i^{(1)}, s_i^{(1)}, o_i^{(1)}) \mid a_j^{(2)} \in \mathcal{A}^{(2)}, i = \mathcal{M}(a_j^{(2)})\}, \quad (7)$$

where  $p_j^{(2)}$  is the fine-level position and the tuple  $(f_i^{(1)}, s_i^{(1)}, o_i^{(1)})$  denotes the decoded attributes inherited from the  $i$ -th coarse-level anchor in  $\mathcal{A}^{(1)}$ . To explicitly capture the geometric relations among

neighboring contexts and model local structure dependencies, we construct a Ball  $k$ -nearest neighbor (Ball  $k$ -NN) graph [42] over  $\mathcal{A}_{pre}^{(2)}$  based on the spatial positions of the fine-level anchors. This graph prior, denoted as  $\mathcal{G}_{geo}^{(2)} = (\mathcal{A}_{pre}^{(2)}, \mathcal{E})$ , where  $\mathcal{E}$  represents the edges connecting spatially neighboring anchors, encapsulates both the inherited coarse-level preliminary contexts and the fine-level local geometric correlations. It provides a structured foundation for subsequent geometry-guided feature refinement in the GG-Conv.

**3) Geometry-Guided Convolution (GG-Conv).** For the graph-based anchor prior  $\mathcal{G}_{geo}^{(2)}$  with its  $k$ -NN graph structure, a straightforward approach is to directly process these retrieved features through a Multi-Layer Perceptron (MLP), as adopted in Context-GS [47]. However, while  $\mathcal{G}_{geo}^{(2)}$  provides a coarse graph-structured contextual priors, simply concatenating them cannot adequately capture the fine-grained geometric correlations in irregular and unstructured anchor distributions. To address this, we propose GG-Conv, which performs adaptive feature refinement upon the local neighborhood. As illustrated in Fig. 4, GG-Conv refines the preliminary features of each query anchor  $a_{i(pre)}^{(2)}$  by aggregating context priors from its  $k$ -NN neighbors  $a_{j(pre)}^{(2)}$  through two cooperative branches.

**Geometry Branch:** To capture local geometric correlations, we compute normalized relative offsets  $\Delta \hat{p}_{ij} = \text{Norm}(p_j - p_i)$  to query a learnable 3D kernel  $\mathbf{T} \in \mathbb{R}^{D \times D \times D \times C}$ . Specifically,  $\Delta \hat{p}_{ij}$  is treated as a continuous query coordinate within the grid space of  $\mathbf{T}$ , from which a dynamic kernel  $w_{ij}$  is retrieved via trilinear interpolation:

$$w_{ij} = \text{Tri-Interp}(\text{Look-up}(\mathbf{T}, \Delta \hat{p}_{ij})) \quad (8)$$

Here  $\text{Tri-Interp}(\cdot)$  interpolates over the eight nearest integer grid cells in  $\mathbf{T}$  to perceive fine-grained geometric variations beyond discrete grid resolutions. This mechanism ensures spatially-continuous weighting for effective geometry-aware feature aggregation.

**Feature Branch:** Concurrently, the feature branch extracts semantic-geometric correlations. Specifically, we first concatenate the residual features  $\Delta \mathbf{f}_{ij} = \mathbf{f}_j - \mathbf{f}_i$  with the relative spatial offsets  $\Delta \mathbf{p}_{ij}$ . The concatenated feature is then transformed via an MLP to extract refined semantic embeddings that are implicitly aware of the local geometry:

$$\mathbf{e}_{ij} = \text{MLP}([\Delta \mathbf{f}_{ij} \parallel \Delta \mathbf{p}_{ij}]) \quad (9)$$

where  $[\cdot \parallel \cdot]$  denotes the concatenation operation. Finally, the dynamic geometric weights from the first branch explicitly modulate these embeddings to produce the geometry-guided context  $\mathbf{f}_{i(ctx)}$ :

$$\mathbf{f}_{i(ctx)} = \sum_{j \in \mathcal{N}(i)} \mathbf{w}_{ij} \odot \mathbf{e}_{ij} \quad (10)$$

where  $\odot$  denotes the element-wise product.

The Local Geometry-Guided Context  $\mathbf{a}_{i(ctx)}$  is formed by concatenating the refined geometry-aware feature  $\mathbf{f}_{i(ctx)}$  with inherited attributes  $(\mathbf{p}_i, \mathbf{s}_i, \mathbf{o}_i)$ . By integrating local neighborhood correlations with global geometric priors,  $\mathbf{a}_{i(ctx)}$  provides a comprehensive representation of the anchor’s state. This  $\mathbf{a}_{i(ctx)}$  is subsequently projected via an MLP to predict distribution parameters:

$$\mu, \sigma, \Delta_{\text{adj}} = \text{MLP}(\mathbf{a}_{i(ctx)}), \quad (11)$$

where  $\mu$  and  $\sigma$  characterize the attribute distribution, and  $\Delta_{\text{adj}}$  adaptively adjusts the quantization step based on local structural complexity. By operating on graph-structured priors, GG-Conv enables spatially-adaptive bitrate allocation, prioritizing complex geometric regions while maintaining high compression efficiency in smoother areas.

### 3.5 Bitstream Composition.

The final bitstream is composed of three parts:  $R = R_{\text{geo}} + R_{\text{attr}} + R_{\text{model}}$ , where  $R_{\text{geo}}$ ,  $R_{\text{attr}}$ , and  $R_{\text{model}}$  denote the bitrate associated with anchor geometry, hierarchical anchor attributes, and model parameters, respectively. Specifically,  $R_{\text{geo}}$  represents the explicit anchor coordinates, which are losslessly compressed after quantization.  $R_{\text{attr}}$  comprises the hierarchical attributes (features, scalings, offsets) of both  $\mathcal{A}^{(1)}$  and  $\mathcal{A}^{(2)}$ , encoded via the proposed hierarchical geometry-guided context modeling.  $R_{\text{model}}$  stores the quantized weights of the shared MLPs and GG-Conv modules as a lightweight model header.

### 3.6 Optimization

The proposed GeoHCC for 3DGS compression is optimized under a rate-distortion objective:

$$\mathcal{L} = \mathcal{L}_{\text{render}} + \lambda \mathcal{L}_{\text{anchor}}, \quad (12)$$

where  $\mathcal{L}_{\text{render}}$  denotes the rendering loss inherited from Scaffold-GS [29] and serves as the distortion term, while  $\mathcal{L}_{\text{anchor}}$  denotes the estimated entropy-coded bitrate of the anchor attributes, including positions, opacities, and feature descriptors, following HAC++ [5] and Context-GS [47], and serves as the rate term. The hyperparameter  $\lambda > 0$  controls the trade-off between reconstruction fidelity ( $\mathcal{L}_{\text{render}}$ ) and compression efficiency ( $\mathcal{L}_{\text{anchor}}$ ).

## 4 Experiments

### 4.1 Implementation Details

We implement GeoHCC within the PyTorch framework, building upon the official Scaffold-GS codebase [29]. To ensure the convergence of geometry-aware components, models are trained for 35,000 iterations. We adopt a minimalist two-level hierarchy ( $L = 2$ ) and set the voxelization scaling factor  $s$  consistent with Context-GS [47]. For local geometry-aware perception via Ball K-NN graph construction, the neighbor count is uniformly fixed at  $K = 8$  for both NAAP and the formation of  $\mathcal{G}_{\text{geo}}^{(2)}$ , while the GG-Conv volumetric kernel size is set to  $k = 5$ . Unless otherwise specified, we follow the default Scaffold-GS configuration, utilizing an anchor feature dimension of 50 and a compressed latent dimension of 12.

### 4.2 Experiment Details

**Datasets.** Our method is evaluated on four standard real-world benchmarks: Mip-NeRF360 [3] (utilizing all 9 scenes), BungeeNeRF [52], DeepBlending [16], and Tanks&Temples [20].

**Baseline Methods.** We compare our method with a wide range of state-of-the-art 3DGS compression approaches, which can be grouped into two main streams. The first focuses on compact representations via parameter pruning or vector quantization, including Scaffold-GS [29], Compressed3D [37], and CompGS [28]. The second stream, more related to our work, improves entropy coding by exploiting contextual priors. Examples include HAC [4] and HAC++ [5], which adopt hash grids for spatial compactness, and Context-GS [47], which models anchor-level context as hyperpriors. More recently, Liu et al. [26] introduced a Mixture-of-Experts (MoE) module for robust feature learning, while CAT-3DGS [55] applies channel-wise autoregressive modeling for attribute compression. We benchmark against these methods to validate the effectiveness of our local geometry-aware hierarchical context modeling.

**Metrics.** We evaluate compression performance in terms of storage size, measured in megabytes (MB). To assess the visual quality of rendered images generated from the compressed 3DGS data, we employ three standard metrics: Peak Signal-to-Noise Ratio (PSNR), Structural Similarity Index (SSIM) [49], and Learned Perceptual Image Patch Similarity (LPIPS) [57].

### 4.3 Experiment Results

**Quantitative Analysis.** As shown in Table 1, our proposed GeoHCC achieves significant improvements over the Scaffold-GS [29] backbone. It delivers an average storage reduction of over 21× while maintaining competitive or even superior rendering fidelity in terms of PSNR and SSIM. Compared with state-of-the-art methods, including HAC [4], HAC++ [5], Context-GS [47], CAT-3DGS [54], and Liu et al. [26], GeoHCC consistently demonstrates better rate-distortion performance, especially at low bitrates. Notably, in several scenes under high-rate settings, GeoHCC even surpasses the uncompressed Scaffold-GS in both PSNR and SSIM. Furthermore, the Rate-Distortion curves in Fig. 6 confirm that GeoHCC provides a superior performance envelope, achieving higher rendering quality at equivalent bitrates across a wide range of compression ratios.

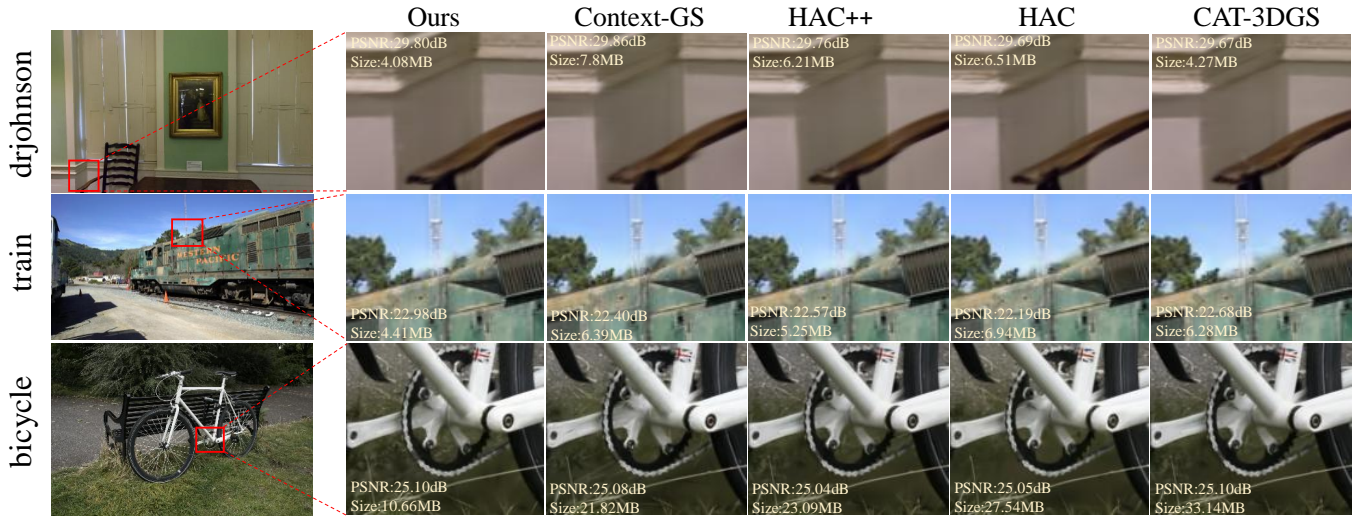


Figure 5: Qualitative results of the proposed method compared to existing compression methods.

Table 1: Comparison against existing compression approaches. Our method is evaluated under two settings: a high-fidelity mode and a high-compression mode, showcasing its versatility. Cells colored **Red** and **yellow** highlight the top-performing and second-best results, respectively, for both the low-bitrate and high-bitrate regimes. All size are reported in MB.

| Datasets<br>Methods        | Mip-NeRF360 [3] |       |        |       | BungeeNeRF [52] |       |        |       | DeepBlending [16] |       |        |       | Tank&Temples [20] |       |        |       |
|----------------------------|-----------------|-------|--------|-------|-----------------|-------|--------|-------|-------------------|-------|--------|-------|-------------------|-------|--------|-------|
|                            | psnr↑           | ssim↑ | lpips↓ | size↓ | psnr↑           | ssim↑ | lpips↓ | size↓ | psnr↑             | ssim↑ | lpips↓ | size↓ | psnr↑             | ssim↑ | lpips↓ | size↓ |
| 3DGS [2]                   | 27.49           | 0.813 | 0.222  | 744.7 | 24.87           | 0.841 | 0.205  | 1616  | 29.42             | 0.899 | 0.247  | 663.9 | 23.69             | 0.844 | 0.178  | 431.0 |
| Scaffold-GS [29]           | 27.50           | 0.806 | 0.252  | 253.9 | 26.62           | 0.865 | 0.241  | 183.0 | 30.21             | 0.906 | 0.254  | 66.00 | 23.96             | 0.853 | 0.177  | 86.50 |
| Compact3DGS [21]           | 27.08           | 0.798 | 0.247  | 48.80 | 23.36           | 0.788 | 0.251  | 82.60 | 29.79             | 0.901 | 0.258  | 43.21 | 23.32             | 0.831 | 0.201  | 39.43 |
| Compressed3D [37]          | 26.98           | 0.801 | 0.238  | 28.80 | 24.13           | 0.802 | 0.245  | 55.79 | 29.38             | 0.898 | 0.253  | 25.30 | 23.32             | 0.832 | 0.194  | 17.28 |
| Morgen. et al. [35]        | 26.01           | 0.772 | 0.259  | 23.90 | 22.43           | 0.708 | 0.339  | 48.25 | 28.92             | 0.891 | 0.276  | 8.40  | 22.78             | 0.817 | 0.211  | 13.05 |
| CompGS [28]                | 27.26           | 0.803 | 0.239  | 16.50 | -               | -     | -      | -     | 29.69             | 0.901 | 0.279  | 8.77  | 23.70             | 0.837 | 0.208  | 9.60  |
| HAC(low-rate) [4]          | 27.53           | 0.807 | 0.238  | 15.26 | 26.48           | 0.845 | 0.25   | 18.49 | 29.98             | 0.902 | 0.269  | 4.35  | 24.04             | 0.846 | 0.187  | 8.10  |
| Context-GS(low-rate) [47]  | 27.62           | 0.778 | 0.237  | 12.68 | 26.90           | 0.866 | 0.222  | 14.00 | 30.11             | 0.907 | 0.265  | 3.43  | 24.20             | 0.852 | 0.184  | 7.05  |
| HAC++(low-rate) [5]        | 27.6            | 0.803 | 0.253  | 8.34  | 26.78           | 0.858 | 0.235  | 11.75 | 30.16             | 0.907 | 0.266  | 2.91  | 24.22             | 0.849 | 0.190  | 5.18  |
| <b>Ours (low-rate)</b>     | 27.64           | 0.805 | 0.247  | 8.23  | 26.93           | 0.866 | 0.231  | 11.59 | 30.25             | 0.909 | 0.267  | 2.83  | 24.32             | 0.852 | 0.187  | 4.92  |
| HAC(high-rate) [4]         | 27.77           | 0.811 | 0.230  | 21.84 | 27.08           | 0.872 | 0.209  | 29.72 | 30.34             | 0.906 | 0.258  | 6.35  | 24.40             | 0.853 | 0.177  | 11.24 |
| HAC++(high-rate) [5]       | 27.82           | 0.811 | 0.231  | 18.48 | 27.17           | 0.879 | 0.196  | 20.82 | 30.34             | 0.911 | 0.254  | 5.287 | 24.32             | 0.854 | 0.178  | 8.63  |
| Context-GS(high-rate) [47] | 27.75           | 0.811 | 0.231  | 18.41 | 27.15           | 0.875 | 0.205  | 21.80 | 30.39             | 0.909 | 0.258  | 6.60  | 24.29             | 0.855 | 0.176  | 11.80 |
| CAT-3DGS [54]              | 27.77           | 0.809 | 0.241  | 12.35 | 27.35           | 0.886 | 0.183  | 26.59 | 30.29             | 0.909 | 0.269  | 3.56  | 24.41             | 0.853 | 0.189  | 6.93  |
| Liu. et al. [26]           | 27.68           | 0.808 | 0.234  | 15.64 | 27.26           | 0.875 | 0.207  | 20.83 | 30.45             | 0.912 | 0.250  | 5.65  | 24.21             | 0.861 | 0.163  | 8.98  |
| <b>Ours (high-rate)</b>    | 27.82           | 0.812 | 0.2351 | 12.24 | 27.46           | 0.883 | 0.196  | 19.48 | 30.49             | 0.912 | 0.250  | 5.63  | 24.43             | 0.856 | 0.177  | 8.49  |

**Qualitative Analysis.** As shown in Figure 5, GeoHCC produces sharper structural details and significantly fewer artifacts compared to both the baseline and competing methods. This improvement stems from our locally geometry-aware constraints, which leverage local geometric context as strong regularization to suppress floaters while enhancing fine local texture details. Thanks to the

geometry-guided context modeling via GG-Conv, our method effectively preserves high-frequency textures even at low bitrates, where other approaches often suffer from blurring or “popping” artifacts.

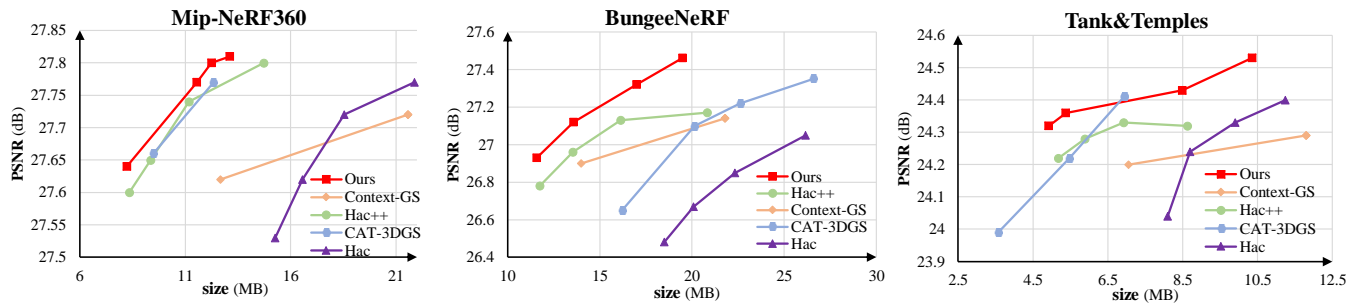


Figure 6: Rate-Distortion (RD) performance curves. Comparison with advanced compression techniques (HAC, HAC++, Context-GS, CAT-3DGS) on the Mip-NeRF360, BungeeNeRF, and Tank&Temples datasets. GeoHCC demonstrates robust coding efficiency, maintaining the upper envelope across a wide range of bitrates.

Table 2: Comparison of storage breakdown (Positions, Features, MLP, Others, “Others” includes auxiliary structures and metadata (e.g., scalings, offsets, masks)), and rendering FPS on the “Bicycle” scene between Context-GS (vanilla EM, i.e., Entropy Modeling) and our GG-Conv-based Hierarchical Geometry-Guided Context EM.

| Methods                       | Storage Costs (MB)↓ |          |        |        |       | Fidelity |        |        | Rendering |
|-------------------------------|---------------------|----------|--------|--------|-------|----------|--------|--------|-----------|
|                               | Positions           | Features | MLP    | Others | Total | PSNR↑    | SSIM↑  | LPIPS↓ | FPS       |
| Vanilla EM [47]               | 5.24                | 8.27     | 0.3162 | 11.24  | 25.07 | 25.07    | 0.7391 | 0.2683 | 135       |
| GG-Conv-based EM(two level)   | 4.69                | 4.51     | 0.2381 | 6.31   | 15.75 | 25.16    | 0.7415 | 0.2704 | 170       |
| GG-Conv-based EM(three level) | 4.66                | 6.82     | 0.3162 | 7.54   | 19.34 | 25.10    | 0.7416 | 0.2703 | 160       |

Table 3: Quantitative ablation study on the Deep Blending dataset. (1) Ours: the full version of our proposed compact neural 3DGS compression framework with both NAAP and GG-Conv. (2) Ours w/o GG-Conv: our method without the GG-Conv component. (3) Ours w/o NAAP: our method without the NAAP component. (4) Ours w/o NAAP & GG-Conv: our method without both proposed components.

| Method                  | PSNR↑        | SSIM↑         | LPIPS↓        | size↓          |
|-------------------------|--------------|---------------|---------------|----------------|
| Ours w/o NAAP & GG-Conv | 30.10        | 0.9062        | 0.2659        | 3.76 MB        |
| Ours w/o GG-Conv        | 30.13        | 0.9087        | 0.2656        | 3.72 MB        |
| Ours w/o NAAP           | 30.20        | 0.9095        | 0.2648        | 3.58 MB        |
| Ours                    | <b>30.31</b> | <b>0.9106</b> | <b>0.2636</b> | <b>3.47 MB</b> |

#### 4.4 Ablation Study and Analysis

**Effectiveness of Different Components.** As shown in Table 3, we conduct an ablation study on the Deep Blending dataset to evaluate the contribution of each proposed component in our GeoHCC framework. Removing NAAP (“Ours w/o NAAP”) leads to a decrease of 0.11 dB in PSNR, 0.001 in SSIM, and a slight increase of 0.11 MB in storage size compared to the full model. Removing GG-Conv (“Ours w/o GG-Conv”) results in a drop of 0.18 dB in PSNR, 0.002 in SSIM, and an additional 0.25 MB in size. When both components are removed (“Ours w/o NAAP & GG-Conv”), the performance degrades further by 0.21 dB in PSNR, 0.004 in SSIM, and 0.29 MB in storage compared to the full model. These results demonstrate that both NAAP and GG-Conv are essential for achieving high rendering quality under strong compression constraints. Notably,

the combined performance gain from NAAP and GG-Conv exceeds the sum of their individual improvements, revealing strong synergy between the two modules. This indicates that NAAP’s preservation of local geometric structures among anchors creates more structured representations that enhance the effectiveness of subsequent hierarchical entropy coding, allowing GG-Conv to achieve superior compression efficiency and rendering quality under tight bit constraints.

Table 4: Storage comparison between vanilla pruning (Context-GS [47]) and our GeoHCC method.

| Method          | Positions (MB) | Features (MB)  |
|-----------------|----------------|----------------|
| Vanilla Pruning | 0.7531         | 1.1108         |
| NAAP (Ours)     | 0.7689 (+2.1%) | 1.0847 (-2.4%) |

**Effectiveness of NAAP.** As shown in Table 4 on the Deep Blending dataset, compared to vanilla pruning [47], NAAP increases positions storage by only 2.1% while reducing features storage by 2.4%. This indicates that NAAP selectively retains a small number of critical anchors to preserve local geometric structures. These anchors enable more coherent local geometry in the gaussian field, which in turn creates stronger spatial correlations among features. End-to-end optimization then exploits this structure to remove redundancy more effectively, allowing significantly better entropy coding of the features. Thus, the tiny anchor overhead is largely compensated by much greater feature compression, revealing that geometry-aware anchor preservation is a highly efficient way to improve structured representation and overall compression in Gaussian splatting.

**Effectiveness of Hierarchical Geometry-Guided Context Modeling.** We evaluate the proposed hierarchical geometry-guided context modeling module against the vanilla entropy model [47] under the same NAAP framework. As shown in Table 2, compared to the baseline, our two-level GG-Conv-based EM significantly reduces the total storage cost from 25.07 MB to 15.75 MB (37.2% reduction) while improving PSNR from 25.07 dB to 25.16 dB. Most notably, the storage for anchor features is nearly halved (from 8.27 MB to 4.51 MB), and the overhead in the "Others" category drops from 11.24 MB to 6.31 MB, demonstrating superior redundancy elimination. We also find that deeper hierarchies do not necessarily enhance efficiency. Although the three-level scheme slightly optimizes position storage (4.66 MB), it increases feature costs to 6.82 MB and total storage to 19.34 MB. This stems from the excessive computational overhead and complex cross-layer dependencies that provide diminishing returns in fidelity. Therefore, we adopt the two-level design. The efficiency of our model is driven by the GG-Conv operator, which leverages local geometric correlations to dynamically weight anchor attributes, producing geometry-aware context. This facilitates the derivation of informed conditional priors with high structural fidelity, which enhances the exploitation of inter-anchor dependencies and ensures a thorough reduction of attribute redundancy in both features and metadata.

## 5 Conclusion

To enhance 3DGS compression performance, we propose a local geometry-aware framework that consistently exploits geometric relationships within anchor neighborhoods. By introducing Neighborhood-Aware Anchor Pruning (NAAP), we achieve a sparse yet locally geometry-consistent hierarchy through adaptive neighbor merging. Building upon this structure, our hierarchical geometry-guided context modeling scheme, powered by the lightweight GG-Conv operator, leverages geometry-guided coarse-to-fine priors to effectively minimize inter-anchor redundancy. Extensive experiments demonstrate that our method achieves state-of-the-art rate-distortion performance, delivering superior rendering quality at substantially reduced storage costs.

## References

- [1] Muhammad Salman Ali, Maryam Qamar, Sung-Ho Bae, and Enzo Tartaglione. 2024. Trimming the fat: Efficient compression of 3d gaussian splats through pruning. *arXiv preprint arXiv:2406.18214* (2024).
- [2] Milena T Bagdasarian, Paul Knoll, Florian Barthel, Anna Hilsmann, Peter Eisert, and Wieland Morgenstern. [n. d.]. 3dgs. zip: a survey on 3D gaussian splatting compression methods (2024). URL <https://arxiv.org/abs/2407.09510> ([n. d.]).
- [3] Jonathan T Barron, Ben Mildenhall, Dor Verbin, Pratul P Srinivasan, and Peter Hedman. 2022. Mip-nerf 360: Unbounded anti-aliased neural radiance fields. In *Proceedings of the IEEE/CVF conference on computer vision and pattern recognition*. 5470–5479.
- [4] Yihang Chen, Qianyi Wu, Weiyao Lin, Mehrtash Harandi, and Jianfei Cai. 2024. Hac: Hash-grid assisted context for 3d gaussian splatting compression. In *European Conference on Computer Vision*. Springer, 422–438.
- [5] Yihang Chen, Qianyi Wu, Weiyao Lin, Mehrtash Harandi, and Jianfei Cai. 2025. Hac++: Towards 100x compression of 3d gaussian splatting. *arXiv preprint arXiv:2501.12255* (2025).
- [6] Kai Cheng, Xiaoxiao Long, Kaizhi Yang, Yao Yao, Wei Yin, Yuexin Ma, Wenping Wang, and Xuejin Chen. 2024. Gaussianpro: 3d gaussian splatting with progressive propagation. In *Forty-first International Conference on Machine Learning*.
- [7] Zhengxue Cheng, Heming Sun, Masaru Takeuchi, and Jiro Katto. 2020. Learned image compression with discretized gaussian mixture likelihoods and attention modules. In *Proceedings of the IEEE/CVF conference on computer vision and pattern recognition*. 7939–7948.
- [8] Xuan Deng, Xingtao Wang, Xiandong Meng, Debin Zhao, and Xiaopeng Fan. 2025. PVINet: Point-Voxel Interlaced Network for Point Cloud Compression. *IEEE Signal Processing Letters* 33 (2025), 61–65.
- [9] Tingyu Fan, Linyao Gao, Yiling Xu, Zhu Li, and Dong Wang. 2022. D-dpcc: Deep dynamic point cloud compression via 3d motion prediction. *arXiv preprint arXiv:2205.01135* (2022).
- [10] Zhiwen Fan, Kevin Wang, Kairun Wen, Zehao Zhu, Dejia Xu, Zhangyang Wang, et al. 2024. Lightgaussian: Unbounded 3d gaussian compression with 15x reduction and 200+ fps. *Advances in neural information processing systems* 37 (2024), 140138–140158.
- [11] Guangchi Fang and Bing Wang. 2024. Mini-splatting: Representing scenes with a constrained number of gaussians. In *European conference on computer vision*. Springer, 165–181.
- [12] Wei Gao, Wenxu Gao, Xingming Mu, Changhao Peng, and Ge Li. 2026. Overview and comparison of avs point cloud compression standard. *arXiv preprint arXiv:2602.08613* (2026).
- [13] Sharath Girish, Kamal Gupta, and Abhinav Shrivastava. 2024. Eagles: Efficient accelerated 3d gaussians with lightweight encodings. In *European Conference on Computer Vision*. Springer, 54–71.
- [14] Zhiyang Guo, Wengang Zhou, Min Wang, Li Li, and Houqiang Li. 2025. Hand-NeRF++: Modeling Animatable Interacting Hands With Neural Radiance Fields. *IEEE Transactions on Pattern Analysis and Machine Intelligence* (2025).
- [15] Dailan He, Yaoyan Zheng, Baocheng Sun, Yan Wang, and Hongwei Qin. 2021. Checkerboard context model for efficient learned image compression. In *Proceedings of the IEEE/CVF Conference on Computer Vision and Pattern Recognition*. 14771–14780.
- [16] Peter Hedman, Julien Philip, True Price, Jan-Michael Frahm, George Drettakis, and Gabriel Brostow. 2018. Deep blending for free-viewpoint image-based rendering. *ACM Transactions on Graphics (ToG)* 37, 6 (2018), 1–15.
- [17] Zhaoyang Jia, Bin Li, Jiahao Li, Wenxuan Xie, Linfeng Qi, Houqiang Li, and Yan Lu. 2025. Towards practical real-time neural video compression. In *Proceedings of the Computer Vision and Pattern Recognition Conference*. 12543–12552.
- [18] Bernhard Kerbl, Georgios Kopanas, Thomas Leimkühler, and George Drettakis. 2023. 3D Gaussian splatting for real-time radiance field rendering. *ACM Trans. Graph.* 42, 4 (2023), 139–1.
- [19] Siyeon Kim, Kyungjin Lee, and Youngki Lee. 2024. Color-cued efficient densification method for 3d gaussian splatting. In *Proceedings of the IEEE/CVF Conference on Computer Vision and Pattern Recognition*. 775–783.
- [20] Arno Knapitsch, Jaesik Park, Qian-Yi Zhou, and Vladlen Koltun. 2017. Tanks and temples: Benchmarking large-scale scene reconstruction. *ACM Transactions on Graphics (ToG)* 36, 4 (2017), 1–13.
- [21] Joo Chan Lee, Daniel Rho, Xiangyu Sun, Jong Hwan Ko, and Eunbyung Park. 2024. Compact 3d gaussian representation for radiance field. In *Proceedings of the IEEE/CVF Conference on Computer Vision and Pattern Recognition*. 21719–21728.
- [22] Jiahao Li, Bin Li, and Yan Lu. 2023. Neural video compression with diverse contexts. In *Proceedings of the IEEE/CVF conference on computer vision and pattern recognition*. 22616–22626.
- [23] Jiahao Li, Bin Li, and Yan Lu. 2024. Neural video compression with feature modulation. In *Proceedings of the IEEE/CVF Conference on Computer Vision and Pattern Recognition*. 26099–26108.
- [24] Han Liu, Hengyu Man, Xingtao Wang, Wenrui Li, and Debin Zhao. 2026. MRT: Learning Compact Representations with Mixed RWKV-Transformer for Extreme Image Compression. In *Proceedings of the AAAI Conference on Artificial Intelligence*, Vol. 40. 10430–10438.
- [25] Lei Liu, Zhenghao Chen, Wei Jiang, Wei Wang, and Dong Xu. 2024. Hemgs: A hybrid entropy model for 3d gaussian splatting data compression. *arXiv preprint arXiv:2411.18473* (2024).
- [26] Lei Liu, Zhenghao Chen, and Dong Xu. 2025. 3D Gaussian Splatting Data Compression with Mixture of Priors. In *Proceedings of the 33rd ACM International Conference on Multimedia*. 8341–8350.
- [27] Rong Liu, Rui Xu, Yue Hu, Meida Chen, and Andrew Feng. 2024. Atomgs: Atomizing gaussian splatting for high-fidelity radiance field. *arXiv preprint arXiv:2405.12369* (2024).
- [28] Xiangrui Liu, Xinju Wu, Pingping Zhang, Shiqi Wang, Zhu Li, and Sam Kwong. 2024. Compgs: Efficient 3d scene representation via compressed gaussian splatting. In *Proceedings of the 32nd ACM International Conference on Multimedia*. 2936–2944.
- [29] Tao Lu, Mulin Yu, Linning Xu, Yuanbo Xiangli, Limin Wang, Dahua Lin, and Bo Dai. 2024. Scaffold-gs: Structured 3d gaussians for view-adaptive rendering. In *Proceedings of the IEEE/CVF Conference on Computer Vision and Pattern Recognition*. 20654–20664.
- [30] Saswat Subhajyoti Mallick, Rahul Goel, Bernhard Kerbl, Markus Steinberger, Francisco Vicente Carrasco, and Fernando De La Torre. 2024. Taming 3dgs: High-quality radiance fields with limited resources. In *SIGGRAPH Asia 2024 Conference Papers*. 1–11.
- [31] Hengyu Man, Xiaopeng Fan, Riyu Lu, Chang Yu, and Debin Zhao. 2024. MetaIP: Meta-network-based intra prediction with customized parameters for video coding. *IEEE Transactions on Circuits and Systems for Video Technology* 34, 10

- (2024), 9591–9605.
- [32] Hengyu Man, Xiaopeng Fan, Ruiqin Xiong, and Debin Zhao. 2023. Tree-Structured Data Clustering-Driven Neural Network for Intra Prediction in Video Coding. *IEEE Transactions on Image Processing* 32 (2023), 3493–3506.
- [33] Hengyu Man, Hao Wang, Riyu Lu, Zhaolin Wan, Xiaopeng Fan, and Debin Zhao. 2025. Content-Aware Dynamic In-Loop Filter With Adjustable Complexity for VVC Intra Coding. *IEEE Transactions on Circuits and Systems for Video Technology* 35, 6 (2025), 6114–6128.
- [34] Ben Mildenhall, Pratul P Srinivasan, Matthew Tancik, Jonathan T Barron, Ravi Ramamoorthi, and Ren Ng. 2021. Nerf: Representing scenes as neural radiance fields for view synthesis. *Commun. ACM* 65, 1 (2021), 99–106.
- [35] Wieland Morgenstern, Florian Barthel, Anna Hilsmann, and Peter Eisert. 2024. Compact 3d scene representation via self-organizing gaussian grids. In *European Conference on Computer Vision*. Springer, 18–34.
- [36] Thomas Müller, Alex Evans, Christoph Schied, and Alexander Keller. 2022. Instant neural graphics primitives with a multiresolution hash encoding. *ACM transactions on graphics (TOG)* 41, 4 (2022), 1–15.
- [37] K Navaneet, Kossar Pourahmadi Meibodi, Soroush Abbasi Koohpayegani, and Hamed Pirsiavash. 2023. Compact3d: Compressing gaussian splat radiance field models with vector quantization. *arXiv preprint arXiv:2311.18159* 2, 3 (2023).
- [38] Simon Niedermayr, Josef Stumpfegger, and Rüdiger Westermann. 2024. Compressed 3d gaussian splatting for accelerated novel view synthesis. In *Proceedings of the IEEE/CVF Conference on Computer Vision and Pattern Recognition*. 10349–10358.
- [39] Antonio Ortega, Pascal Frossard, Jelena Kovačević, José MF Moura, and Pierre Vanderghenst. 2018. Graph signal processing: Overview, challenges, and applications. *Proc. IEEE* 106, 5 (2018), 808–828.
- [40] Panagiotis Papanatakis, Georgios Kopanas, Bernhard Kerbl, Alexandre Lanvin, and George Drettakis. 2024. Reducing the memory footprint of 3d gaussian splatting. *Proceedings of the ACM on Computer Graphics and Interactive Techniques* 7, 1 (2024), 1–17.
- [41] Charles R Qi, Hao Su, Kaichun Mo, and Leonidas J Guibas. 2017. Pointnet: Deep learning on point sets for 3d classification and segmentation. In *Proceedings of the IEEE conference on computer vision and pattern recognition*. 652–660.
- [42] Charles Ruizhongtai Qi, Li Yi, Hao Su, and Leonidas J Guibas. 2017. Pointnet++: Deep hierarchical feature learning on point sets in a metric space. *Advances in neural information processing systems* 30 (2017).
- [43] Kerui Ren, Lihan Jiang, Tao Lu, Mulin Yu, Linning Xu, Zhangkai Ni, and Bo Dai. 2024. Octree-gs: Towards consistent real-time rendering with lod-structured 3d gaussians. *arXiv preprint arXiv:2403.17898* (2024).
- [44] Xihua Sheng, Jiahao Li, Bin Li, Li Li, Dong Liu, and Yan Lu. 2022. Temporal context mining for learned video compression. *IEEE Transactions on Multimedia* 25 (2022), 7311–7322.
- [45] Seunghoo Shin, Jaesik Park, and Sunghyun Cho. 2025. Locality-aware gaussian compression for fast and high-quality rendering. *arXiv preprint arXiv:2501.05757* (2025).
- [46] Heman Wang, Hanxin Zhu, Tianyu He, Runsen Feng, Jiajun Deng, Jiang Bian, and Zhibo Chen. 2024. End-to-end rate-distortion optimized 3d gaussian representation. In *European Conference on Computer Vision*. Springer, 76–92.
- [47] Yufei Wang, Zhihao Li, Lanqing Guo, Wenhan Yang, Alex Kot, and Bihan Wen. 2024. Contextgs: Compact 3d gaussian splatting with anchor level context model. *Advances in neural information processing systems* 37 (2024), 51532–51551.
- [48] Yue Wang, Yongbin Sun, Ziwel Liu, Sanjay E Sarma, Michael M Bronstein, and Justin M Solomon. 2019. Dynamic graph cnn for learning on point clouds. *ACM Transactions on Graphics (tog)* 38, 5 (2019), 1–12.
- [49] Zhou Wang, A.C. Bovik, H.R. Sheikh, and E.P. Simoncelli. 2004. Image quality assessment: from error visibility to structural similarity. *IEEE Transactions on Image Processing* 13, 4 (2004), 600–612. doi:10.1109/TIP.2003.819861
- [50] Zhitao Wang, Hengyu Man, Wenrui Li, Xingtao Wang, Xiaopeng Fan, and Debin Zhao. 2026. T-GVC: Trajectory-Guided Generative Video Coding at Ultra-Low Bitrates. In *Proceedings of the AAAI Conference on Artificial Intelligence*, Vol. 40. 7141–7149.
- [51] Tong Wu, Yu-Jie Yuan, Ling-Xiao Zhang, Jie Yang, Yan-Pei Cao, Ling-Qi Yan, and Lin Gao. 2024. Recent advances in 3d gaussian splatting. *Computational Visual Media* 10, 4 (2024), 613–642.
- [52] Yuanbo Xiangli, Linning Xu, Xingang Pan, Nanxuan Zhao, Anyi Rao, Christian Theobalt, Bo Dai, and Dahua Lin. 2022. Bungeenerf: Progressive neural radiance field for extreme multi-scale scene rendering. In *European conference on computer vision*. Springer, 106–122.
- [53] Runyi Yang, Zhenxin Zhu, Zhou Jiang, Baijun Ye, Xiaoxue Chen, Yifei Zhang, Yuantao Chen, Jian Zhao, and Hao Zhao. 2024. Spectrally pruned gaussian fields with neural compensation. *arXiv preprint arXiv:2405.00676* (2024).
- [54] Yu-Ting Zhan, Cheng-Yuan Ho, Hebi Yang, Yi-Hsin Chen, Jui Chiu Chiang, Yu-Lun Liu, and Wen-Hsiao Peng. 2025. CAT-3DGS: A context-adaptive triplane approach to rate-distortion-optimized 3DGS compression. *arXiv preprint arXiv:2503.00357* (2025).
- [55] Yu-Ting Zhan, Cheng-Yuan Ho, Hebi Yang, Yi-Hsin Chen, Jui Chiu Chiang, Yu-Lun Liu, and Wen-Hsiao Peng. 2025. CAT-3DGS: A context-adaptive triplane approach to rate-distortion-optimized 3DGS compression. In *Proceedings of the Thirteenth International Conference on Learning Representations (ICLR)*.
- [56] Qiang Zhang, Seung-Hwan Baek, Szymon Rusinkiewicz, and Felix Heide. 2022. Differentiable point-based radiance fields for efficient view synthesis. In *SIG-GRAPH Asia 2022 Conference Papers*. 1–12.
- [57] Richard Zhang, Phillip Isola, Alexei A Efros, Eli Shechtman, and Oliver Wang. 2018. The unreasonable effectiveness of deep features as a perceptual metric. In *Proceedings of the IEEE conference on computer vision and pattern recognition*. 586–595.
- [58] Wenkang Zhang, Yan Zhao, Qiang Wang, Zhixin Xu, Li Song, and Zhengxue Cheng. 2026. D-fcgs: Feedforward compression of dynamic gaussian splatting for free-viewpoint videos. In *Proceedings of the AAAI Conference on Artificial Intelligence*, Vol. 40. 16361–16369.